



Attachment No. 3

Summary of Professional Accomplishments

Table of content

1. Names and surname	3
2. Education and degrees	4
3. Information on employment	5
4. Description of the achievements	6
4.1. Title and list of publications constituting the scientific achievement.....	6
4.2. Introduction	7
4.3. Description of the research results presented in publications [H1] – [H6]	11
4.4. Main achievements – summary.....	29
4.5. An importance of publications [H1] – [H6] for the development of GaN nanowires growth technology.....	30
5. Presentation of significant scientific or artistic activity carried out at more than one university, scientific or cultural institution, especially at foreign institutions	33
6. Presentation of teaching and organizational achievements as well as achievements in popularization of science	36
7. Description of scientific achievements unrelated to the topic of habilitation	38
8. References	41

1. Names and surname

Marta Maria Sobańska

ResearcherID: [Q-8669-2016](https://orcid.org/0000-0002-7225-9236)

OrcidID: [0000-0002-7225-9236](https://orcid.org/0000-0002-7225-9236)

2. Education and degrees

(Diplomas, degrees conferred in specific areas of science or arts, including the name of the institution which conferred the degree, year of degree conferment, title of the PhD dissertation)

- 2017/07/04 PhD degree in Electronics
Institute of Electron Technology in Warsaw
title of the thesis: *Wzrost i właściwości nanodrutów azotku galu otrzymanywanych metodą MBE z plazmowym źródłem azotu (Plasma-assisted MBE growth and properties of gallium nitride nanowires)*
Supervisor: prof. dr. hab. Zbigniew R. Żytkiewicz
- 2007/10 – 2009/06 Master of Science in Physics
Cardinal Stefan Wyszyński University in Warsaw
title of the thesis: *Samoorganizujący się wzrost nanometrowych wysp Au na powierzchni Mo (Self-organized growth of Au islands on Mo substrates)*
Supervisor: prof. dr. hab. Andrzej Wawro
- 2004/10 – 2007/06 Bachelor of Science in Applied Informatics
Cardinal Stefan Wyszyński University in Warsaw
title of the thesis: *Bo liczy się reflex (Reflex matters)*
Supervisor: prof. dr. hab. Magdalena Załuska-Kotur

3. Information on employment

2021/04/01 – present	Institute of Physics of Polish Academy of Sciences in Warsaw <i>position:</i> assistant professor
2019/04/01 – 2021/03/31	Institute of Physics of Polish Academy of Sciences in Warsaw <i>position:</i> assistant
2017/09/01 – 2019/03/31	Institute of Physics of Polish Academy of Sciences in Warsaw <i>position:</i> specialist
2010/01/01 – 2017/08/31	Institute of Physics of Polish Academy of Sciences in Warsaw <i>position:</i> technical staff

4. Description of the achievements

4.1. Title and list of publications constituting the scientific achievement

The scientific achievement entitled

Mechanisms of spontaneous crystallization of GaN nanowires by molecular beam epitaxy on amorphous substrates

consists of the following series of thematically related scientific articles published in international journals:

- [H1] **M. Sobanska**, Z.R. Zykiewicz, G. Calabrese, L. Geelhaar, S. Fernández-Garrido
Comprehensive analysis of the self-assembled formation of GaN nanowires on amorphous Al_xO_y : in situ quadrupole mass spectrometry studies
Nanotechnology 30 (2019) 154002
<https://doi.org/10.1088/1361-6528/aafe17>
- [H2] K. Lawniczak-Jablonska, Z.R. Zykiewicz, S. Gieraltowska, **M. Sobanska**, P. Kuzmiuk, K. Klosek
Chemical bonding of nitrogen formed by nitridation of crystalline and amorphous aluminum oxide studied by x-ray photoelectron spectroscopy
RSC Advances 10 (2020) 27932–27939
<http://dx.doi.org/10.1039/d0ra05104g>

- [H3] **M. Sobanska**, Z.R. Zytkeiwicz, K. Klosek, R. Kruszka, K. Golaszewska, M. Ekielski, S. Gieraltowska
Selective area formation of GaN nanowires on GaN substrates by the use of amorphous Al_xO_y nucleation layer
Nanotechnology 31 (2020) 184001
<http://dx.doi.org/10.1088/1361-6528/ab6bf2>
- [H4] **M. Sobanska**, Z.R. Zytkeiwicz, M. Ekielski, K. Klosek, A.S. Sokolovskii, V.G. Dubrovskii
Surface Diffusion of Gallium as the Origin of Inhomogeneity in Selective Area Growth of GaN Nanowires on Al_xO_y Nucleation Stripes
Crystal Growth & Design 20 (2020) 4770–4778
<http://dx.doi.org/10.1021/acs.cgd.0c00530>
- [H5] **M. Sobanska**, N. Garro, K. Klosek, A. Cros, Z.R. Zytkeiwicz
Influence of Si substrate preparation procedure on polarity of self-assembled GaN nanowires on Si(111): Kelvin Probe Force Microscopy studies
Electronics 9 (2020) 1904
<http://dx.doi.org/10.3390/electronics9111904>
- [H6] A. Wierzbicka, G. Tchutchulashvili, **M. Sobanska**, K. Klosek, R. Minikayev, J.Z. Domagala, J. Borysiuk, Z.R. Zytkeiwicz
Arrangement of GaN nanowires on Si(001) substrates studied by X-ray diffraction: Importance of silicon nitride interlayer
Applied Surface Science 425 (2017) 1014–1019
<http://dx.doi.org/10.1016/j.apsusc.2017.07.075>

4.2. Introduction

Rapid progress of nanotechnology has allowed to control the structure of solids nearly in atomic scale. Since reduction of dimensionality results in new interesting properties of materials, this leads to new functionalities of devices based on nanostructures. In particular, nanowires (NWs), which are one-dimensional crystalline objects, have received much

attention as promising building blocks of new devices. Due to their shape and small footprint on a substrate the elastic relaxation of lattice mismatch strain is much easier in NWs. Therefore, even in NWs containing segments of high lattice mismatched materials no dislocations are observed [1]. Moreover, during growth of polar materials on nonpolar substrates (e.g. III-V on Si) generation of antiphase boundaries is much more difficult [2, 3]. As the result, complicated nanostructures with high structural quality, not achievable in planar counterparts, can be obtained. This is crucial for application of heterostructures in efficient electronic and optoelectronic devices as well as in biosensors.

As for the materials of choice, semiconducting nitrides of group III metals, e.g. GaN, are very promising. GaN is an important semiconductor with direct and wide bandgap ($E_g = 3.4$ eV at room temperature). Its alloys with AlN and InN allow light emission from infrared ($E_g = 0.64$ eV for InN) up to ultraviolet ($E_g = 6.2$ eV for AlN). There are no other direct bandgap material system that could be used for light emitters in so wide spectral range. For example GaN/InGaN/AlGaN heterostructures have been used to fabricate infrared, visible or UV LED devices [4 – 7], laser diodes [8, 9], as well as UV photodetectors [10, 11].

Generally, there are two concepts used for fabrication of NWs: *top-down approach* in which the nanowires are cut out (by etching or thermal decomposition) from respective planar structures with masked surface [12, 13] or *bottom-up approach*, when the nucleation and growth conditions are adjusted to force on the substrate growth of NWs instead of planar layer. Since in the former case elimination of defects generated during growth of planar heterostructures as well as during their processing is very difficult [14], a direct crystallization methods offering natural mechanisms of lattice mismatch strain relaxation are preferred.

The most popular techniques applied for growth of group III – V NWs make use of spontaneous formation of GaN nuclei from a gaseous phase on a substrate (*self-induced mode*) or nucleation mechanisms induced by a foreign catalyst particles in *vapor-liquid-solid* (VLS) or *vapor-solid-solid* (VSS) modes. There are literature reports that Ni islands are efficient catalyst centers for GaN NW growth by plasma-assisted molecular beam epitaxy (PAMBE). Nickel droplets effectively capture Ga and N atoms from molecular beams, which leads to supersaturation of the catalyst, crystallization of GaN at bottom of the droplet and consequently to the one-dimensional growth of the nanowire [15]. This is a very efficient growth method. However, a significant incorporation of Ni dopant to GaN [16] results in high concentration of stacking faults, strong nonradiative recombination and low photoluminescence intensity [17]. Thus, catalyst-free growth method developed in 1979 by groups of prof. Katsumi Kishino [18, 19] and prof. Enrique Calleja [20, 21] attracts much

more attention. Since its discovery, the catalyst-free growth method has been used by many groups worldwide with the main focus on the GaN NW growth on silicon substrates. It is mentioning worthy here that the commonly used term *growth of GaN nanowires on Si substrate* is not precise and sometimes misleading. As it is well known, Ga-N bond energy (2.17 eV/bond [22]) is smaller than for Si-N bond (4.6 eV/bond [23]). This means that simultaneous exposure of Si substrate to both Ga and N fluxes must lead to a competition between surface processes of SiN_x formation and nucleation of GaN. Both processes are active until all Si-N bonds are saturated and the surface is covered by a thin SiN_x film on top of which (not directly on Si) the nanowires form. It is well known that competitive nitrogen bonding to Si and Ga results in larger roughness of the SiN_x film, and consequently in increased spatial misorientation of NWs [24]. Therefore, in earlier works we have proposed to separate step of Si substrate nitridation from subsequent growth of GaN. This has been achieved by exposing a deoxidized substrate first to the flux of active nitrogen to create a continuous ~2 nm thick SiN_x film. Only then the Ga source is opened to start GaN nucleation [B13]. In this way independently on GaN growth parameters the fabrication, and thus properties, of the SiN_x buffer layer could be controlled allowing adjustment of arrangement of nanowires on the substrate [B13].

As mentioned already, nitridated silicon is the most common substrate for GaN NW growth. However, applicability of Si substrates is limited (e.g. due to a strong absorption of visible light in silicon), while the use of nonconventional substrate materials (amorphous buffer layers, metals, 2D van der Waals materials, etc.) and their specific properties (electronic and optical) offers new functionalities of semiconductor structures based on NWs. Recent literature reports show that this is the mainstream of current research. Despite that the in-depth understanding of mechanism of self-induced nucleation of GaN NWs on various substrates is still missing. Without that precise control of properties of NW arrays is very difficult and often relies on the low efficient trial and error method.

Deeper insight into the mechanisms active during the self-induced nucleation and PAMBE growth of GaN NWs on non-crystalline substrates is the main goal of the series of scientific articles constituting my habilitation achievement. In my opinion, it is crucial to understand the impact of microstructure of the substrate (or buffer layer) on nucleation kinetics and properties of NWs. Beside importance for basic research it would give more freedom of choosing the substrate according to the needs of a specific device and allow growing on it nanowires with required properties.

The aims of my research in that field performed after PhD thesis defense were:

1. to get deeper understanding of an impact an amorphous substrate has on kinetics of self-induced nucleation of GaN NWs by performing the comprehensive analysis of dependence of NW incubation time on the PAMBE growth conditions on a-Al_xO_y nucleation layer and comparison with similar dependence for standard nitridated Si substrate – *results presented in [H1]*;
2. to develop efficient ways of controlling incubation time of GaN NWs by the choice of substrate and adjustment of the growth conditions – *results presented in [H1]*;
3. to clarify a nature of nucleation centers inducing formation of GaN NWs on a-Al_xO_y nucleation layer by studies of mechanisms of nitrogen incorporation into a-Al_xO_y buffer during its annealing in nitrogen plasma – *results presented in [H2]*;
4. to develop technology and optimize PAMBE growth conditions of selective area formation of GaN NWs on nucleation layer – *results presented in [H3] and [H4]*
5. to clarify an origin of mixed polarity of GaN NWs on silicon substrates – *results presented in [H5]*;
6. to determine an influence of residual surface contamination on the growth mechanism and spatial orientation of GaN NWs on Si(001) substrates – *results presented in [H6]*.

The importance of these topics was highlighted in my PhD thesis already. However, the respective works were performed after defense of the thesis that was devoted to application of a reflection high-energy electron diffraction (RHEED) and a quadrupole mass spectroscopy (QMS) techniques for analysis of nucleation kinetics of GaN NWs and studies of their properties. The exception is the first work on which was initiated in the framework of my PhD thesis preparation. However, in our earlier report [B26] the impact of nitrogen flux on nucleation kinetics was neglected while as recently shown by us in [H1], it significantly influences incubation, nucleation and growth rates. Similarly, the effect of Ga desorption from NW array was completely neglected at that time. In that sense only the experimental results published in [H1] allowed the complete analytical description of incubation time dependence on all PAMBE growth parameters. As will be shown in Section 4.3 this was an essential first step to elaborate effective tools for controlling of NW incubation on a-Al_xO_y buffers. This

was also a precondition for a construction of growth diagrams predicting values of incubation time under growth conditions not explored experimentally and then their comparison with those on standard nitridated Si substrates.

Below results reported in articles [H1] – [H6] are presented in detail. They are summarized in Section 4.4. Next, Section 4.5 shows a significant impact of those results on progress of our research on growth physics and application of GaN NW arrays.

4.3. Description of the research results presented in publications [H1] – [H6]

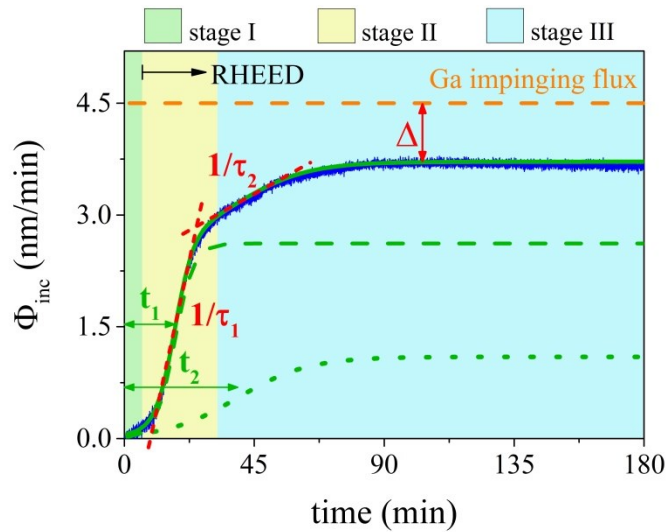


Fig. 1. Temporal evolution of the incorporated Ga flux Φ_{inc} during the growth of a GaN NW ensemble on an $a\text{-Al}_x\text{O}_y$ buffered Si(111) substrate (blue line). The arrow in the upper left corner indicates the time at which the first GaN-related spots became visible in the RHEED pattern. The solid green line shows the best fit of the data by equation (1), which consists of two logistic functions. The individual contributions of the two different logistic functions are shown as green dashed and dotted lines. The dashed red lines illustrate the meaning of the parameters τ_1 and τ_2 in equation (1). The average delay times for the onset of NW formation and the collective effects, t_1 and t_2 , respectively, are marked by double arrows. The temporal evolution Φ_{inc} is divided into three different stages, as indicated in the figure. Δ represents the desorbing Ga flux during the elongation of the GaN NWs. Figure from [H1].

The most important in the series is the article [H1] that presents results of our comprehensive analysis of nucleation of GaN NWs by PAMBE on amorphous $a\text{-Al}_x\text{O}_y$ buffer deposited on Si substrate. The growth was carried out in self-induced mode under N-rich conditions, i.e. when Ga flux controls the GaN growth rate. The main analytical tool was mass quadrupole spectrometer QMS that measured the part of impinging Ga flux that was not incorporated into GaN and desorbed from the substrate. Knowing value of the impinging

Ga flux the quantitative information on Ga incorporation rate to GaN, i.e. on GaN nucleation and NW growth rates, can be inferred from the QMS signal. Fig. 1 shows the typical shape of temporal change of the QMS signal measured during the PAMBE growth of GaN nanowires on a-Al_xO_y buffer (full blue line). In our earlier work [B26] we showed that nucleation and PAMBE growth of GaN NWs proceeds in the following three stages: (i) incubation preceding appearance of 3D GaN nuclei, (ii) formation of semispherical nuclei and their transformation into NW shape, and (iii) follow-up anisotropic growth of NWs, equilibration of their lengths due to a collective effects and eventually coalescence of neighboring NWs. These stages are marked by respective colors in Fig. 1 (*stage I, II, III*). It is mentioning worthy that the same sequence of stages was observed during PAMBE growth of GaN NWs on nitridated Si substrates [25]. Thus our studies show that this type of NW formation is not limited to a particular substrate but is general in nature and inherent to GaN growth by PAMBE. As such it should be transferable to numerous types of substrates

We have shown in our earlier report [B26] that temporal evolution of the Ga flux incorporated to the crystal Φ_{inc} is well described by the sum of two logistic functions according to the equation:

$$\Phi_{inc} = \frac{R_1}{1+\exp\left(-\frac{t-t_1}{\tau_1}\right)} + \frac{R_2}{1+\exp\left(-\frac{t-t_2}{\tau_2}\right)}, \quad (1)$$

where t_1 and $1/\tau_1$ are average nucleation delay time (incubation time) and the time constant of the nucleation rate, respectively. Analogously, t_2 and $1/\tau_2$ parameters represent time delay of the onset of collective effects and a rate constant that reflects the temporal variation in the contribution of collective effects to the total deposition rate, respectively. Values of those parameters are marked in Fig. 1 together with separate contributions of the first and the second logistic functions (green dashed and dotted lines) and the full fit of the QMS profile by Eq. 1 (full green line).

For an analysis of the self-induced nucleation of NWs on various substrates the crucial is the incubation stage when Ga adatoms migrate on the substrate surface until GaN nuclei exceeding the critical size, and thus being thermodynamically stable and able to incorporate next Ga adatoms, are formed. Therefore in [H1] we focused in detail just on this stage. To this end, a series of growth experiments was performed under various growth conditions (growth temperature and Ga and N fluxes), the aim being to determine dependence of the incubation time t_1 for GaN NWs on a-Al_xO_y buffers on all parameters of the growth process. Values of

the incubation time were measured by fitting QMS profiles with the formula (1). For comparison, similar growth experiments were performed on standard nitridated Si substrates (SiN_x/Si). Experimental results obtained for a wide range of growth parameters are shown in Fig. 2.

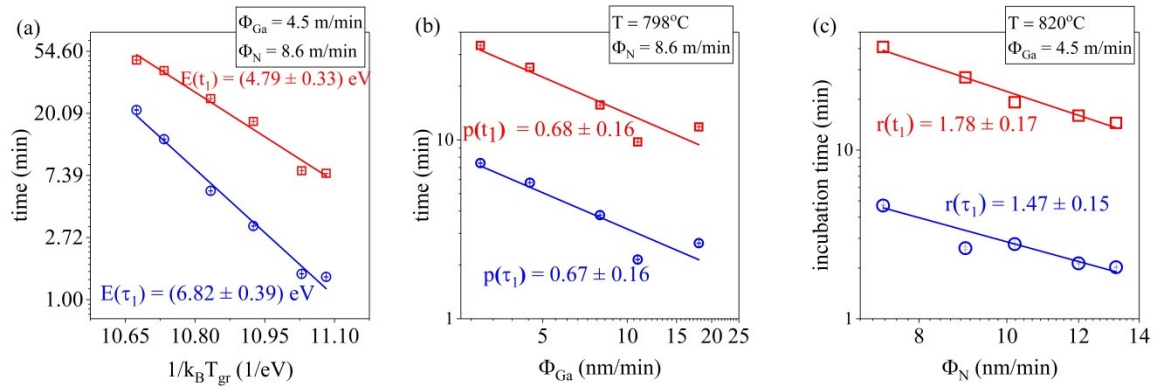


Fig. 2. Dependences of GaN NW incubation time on a- Al_xO_y buffers on (a) growth temperature, (b) Ga flux and (c) N flux. Figure from [H1].

Importantly, we have shown that the experimental data can be well described by the following analytical expression:

$$t_1 = C \times \Phi_N^{-r(t_1)} \times \Phi_{Ga}^{-p(t_1)} \times \exp\left(\frac{-E(t_1)}{k_B T_{gr}}\right), \quad (2)$$

where k_B is the Boltzmann constant, T_{gr} growth temperature, $E(t_1)$ nucleation energy and C is a constant. Using equation (2) and the data shown in Fig. 2 it was possible to determine values of E , p and r parameters characteristic for self-induced nucleation of GaN NWs on a- Al_xO_y by PAMBE. Moreover, this allowed prediction of incubation time value on such substrate for growth conditions not explored experimentally as well as development of efficient ways of controlling the NW incubation stage. As example, Fig. 3 shows calculated from Eq. (2) growth diagrams that help to visualize the impact of growth temperature and Ga flux on incubation time of GaN NWs on (a) SiN_x/Si and (b) a- Al_xO_y substrates. Comparison of data in these diagrams shows that under the same growth conditions incubation time on SiN_x/Si is up to several times longer than on a- Al_xO_y indicating potentially different nucleation mechanisms on both substrates as will be discussed later. It should be noted here that so large differences of GaN incubation times indicates a large potential of using both materials for selective area growth (SAG) of nanowires in the configuration, in which SiN_x masks a substrate while

a-Al_xO_y is a NW nucleation layer. Respective examples will be discussed later on when presenting results of our work [H4].

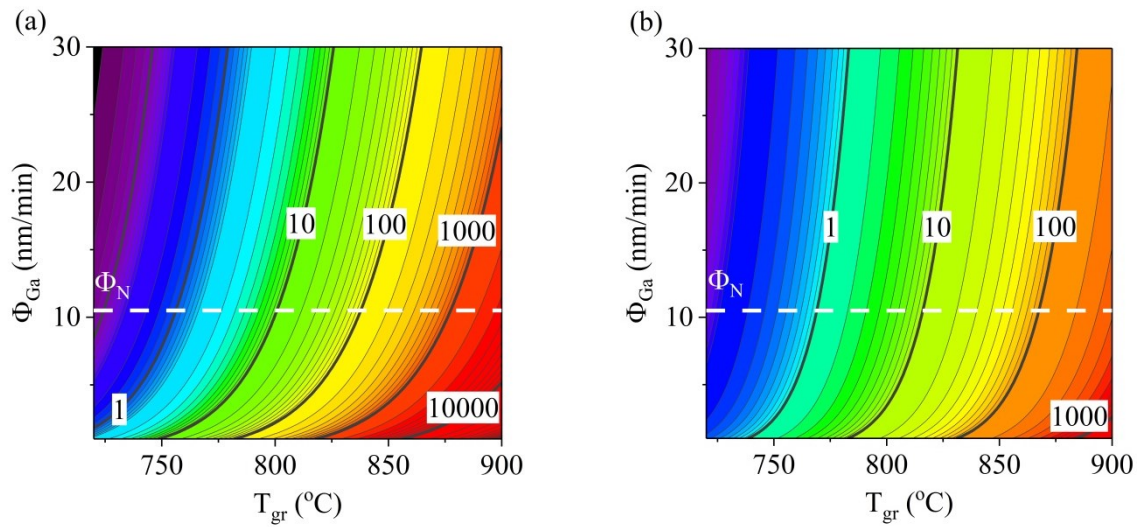


Fig. 3. (a) Growth diagram presenting the impact of the substrate temperature and the impinging Ga flux for a given active N flux (indicated by the white dashed line) on the incubation time t_l for GaN NWs grown on nitridated Si. (b) Growth diagram illustrating the dependence of the incubation time t_l on the substrate temperature and the Ga flux in the case of GaN NWs grown on a-Al_xO_y buffered Si. The values of t_l are displayed as contour plots with a logarithmic scale. The same color scale is used in all diagrams. Figure from [H1].

Results shown in Fig. 3 indicate that on both substrates faster GaN incubation can be obtained by reducing the growth temperature or by increasing the impinging Ga flux. Similarly, we have shown that an increase of active nitrogen flux decreases the incubation time, although this solution is technically more complicated. These conclusions are important, also from application point of view. At high growth temperatures required for exceptional optical properties of NWs [26] GaN incubation on SiN_x/Si substrates can take up to a few hours which implies low growth efficiency at high costs. Thus, elaboration of procedures that could make the incubation stage shorter (e.g. by increasing Ga flux or use of more efficient nucleation layer) is very important.

Analysis of NW nucleation kinetics described above has led us to construction of a growth map illustrating the different growth regimes, namely *planar layer*, *NWs* and *no growth*, that can be obtained when GaN is grown on a-Al_xO_y as a function of the substrate temperature and the impinging Ga flux for a given active N flux (Fig. 4). The boundaries between different regions on the map were calculated from eq. (2) assuming that for the *no growth* region GaN incubation time was longer than three hours making such growth conditions impracticable. The blue *compact layer/NW* boundary was calculated taking into account that the planar layer forms when the *effective* (i.e. corrected for Ga desorption from

the substrate) value of the Ga/N flux ratio was ≥ 1 . The shape of both boundaries on the map was verified experimentally by performing growth experiments under various conditions, post-growth checking surface morphology of the samples by SEM and then by marking the respective points on the map. As seen in Fig.4 the growth conditions for both NW arrays (blue circles) as well as planar GaN layers (red squares) and samples with incubation longer than 3h (green diamonds) are in a perfect agreement with results of calculations. Although the growth map shown in Fig. 4 holds quantitatively only for the given N flux value ($\Phi_N = 8.6$ nm/min), it gives a clear idea on how to control the formation of GaN NWs on a-Al_xO_y buffers layers. Moreover, our results presented in [H1] clearly show that a-Al_xO_y buffer is preferred over the commonly used nitridated Si substrate since it offers shorter incubation times and wider growth window for the formation of GaN NWs.

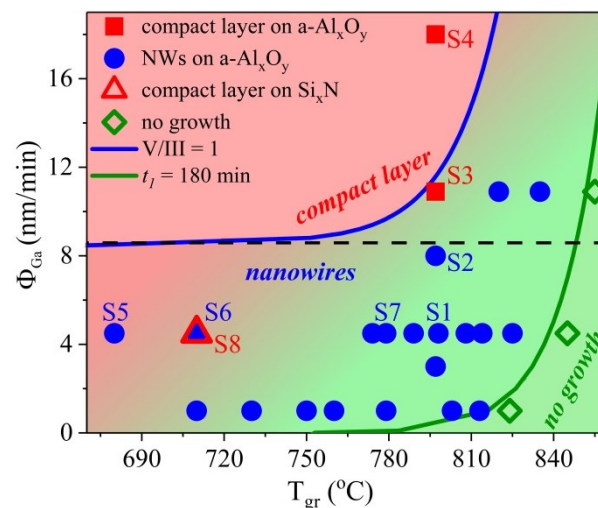


Fig. 4. Growth diagram showing the boundaries between the *compact layer*, *NW*, and *no growth* regimes as a function of impinging Ga flux and the substrate temperature for an active N flux of 8.6 nm min^{-1} . The *NW/no growth* boundary (green line) is calculated according to equation (2) imposing a value of t_l equal to 180 min. Solid symbols show the growth conditions of GaN samples with a NW (blue dots) or a compact layer (red squares) morphology as derived from the inspection of scanning electron micrographs. The green diamonds indicate samples for which we measured an incubation time longer than 180 min. The red triangle indicates the growth conditions employed for the growth of a reference sample on a nitridated Si(111) substrate. The horizontal dashed line indicates the N flux level. Figure from [H1].

The findings presented above raised the fundamental question about the origin of easier nucleation of GaN NWs on amorphous a-Al_xO_y buffer than on SiN_x layer formed during nitridation of Si substrate in nitrogen plasma inside the MBE growth chamber. As shown in our earlier paper [B27] GaN nucleation rate on SiN_x/Si is limited by concentration of Ga adatoms and their surface diffusion rate. However, for a-Al_xO_y substrate dependence of

incubation time on the impinging Ga flux (i.e. value of the p parameter introduced in [H1]) indicates that in this case more efficient is heterogeneous GaN nucleation on foreign nucleation centers. If so, the nucleation rate should be limited by concentration of those centers and their ability to capture Ga adatoms. Presence of such centers in a- Al_xO_y buffer might also explain our earlier observation that under the conditions when on crystalline Al_2O_3 substrate a planar GaN layer forms, on a- Al_xO_y buffer GaN NWs grow [B18]. Intensive studies of a- Al_xO_y buffers by Atomic Force Microscopy (AFM) and Transmission Electron Microscopy (TEM) techniques have not revealed any structural imperfections that could locally favor crystallization of GaN (as for example voids in SiO_2 that are known to induce Ga-assisted formation of GaAs NWs [27]). Thus we assumed that local nonuniformities of chemical composition might play the role of nucleation centers and an analysis of chemical composition uniformity of the a- Al_xO_y buffers by X-ray Photoelectron Spectroscopy (XPS) was performed [H2]. It is well known that during annealing of crystalline sapphire substrates in ammonia flow at high temperatures ($\sim 1050^\circ\text{C}$) prior to GaN epitaxy by Metalorganic Vapor Phase Epitaxy (MOVPE) technique AlN islands appear on the substrate surface allowing easier nucleation of GaN [28]. Therefore we focused on mechanisms of nitrogen incorporation to thin a- Al_xO_y buffers on Si (a- $\text{Al}_x\text{O}_y/\text{Si}$) and Al_2O_3 (a- $\text{Al}_x\text{O}_y/\text{Al}_2\text{O}_3$) as well as to bulk crystalline substrates for comparison. The samples were annealed in nitrogen plasma inside the MBE growth chamber under the same conditions as used for incubation of GaN NWs.

Fig. 5 shows the total amount of nitrogen incorporated to the solid as a function of nitridation time at 800°C . Interestingly, nitrogen uptake by amorphous a- Al_xO_y buffer is easier than by bulk crystalline Al_2O_3 indicating potentially different mechanisms of N incorporation in both cases. However, unexpected is the observation that nitrogen content in the buffer depends on the substrate on which the buffer is deposited: N content in a- $\text{Al}_x\text{O}_y/\text{Si}$ is significantly larger than in buffers deposited on sapphire (a- $\text{Al}_x\text{O}_y/\text{Al}_2\text{O}_3$). In order to determine chemical bonding of nitrogen the N 1s XPS line was studied in detail. Fig. 6 shows as example the shape of this line in a- $\text{Al}_x\text{O}_y/\text{Si}$ sample nitridated for 80 min. The line was deconvoluted into three components with binding energies corresponding to hexagonal AlN, oxinitride AlN-O and $\text{Al}(\text{NO}_y)_x$ rock salt phase containing bonded NO_x molecules. Importantly, the last phase is present in nitridated a- Al_xO_y buffers while it was absent in nitridated crystalline sapphire samples. We have explained the observed differences of N uptake mechanisms by taking into account differences of initial stoichiometry of the samples. At the surface of crystalline sapphire O vacancies were found before nitridation,

which are considered to be necessary for formation of AlN-type bonding by replacement of oxygen atoms by nitrogen. In contrast, in $a\text{-Al}_x\text{O}_y$ films Al vacancies were present at the surface before nitridation, which created new efficient way of N incorporation by nitrogen accumulation in empty octahedral Al vacancies surrounded by O atoms and formation of the $\text{Al}(\text{NO}_y)_x$ phase. For example, in the case of $y = 3$ and $x = 3$ each Al atom is bonded with three NO_3 molecules. Since each N atom bonds to more than one O atom creation of the $\text{Al}(\text{NO}_y)_x$ phase efficiently reduces O excess and oxygen vacancies are formed allowing further incorporation of nitrogen via creation of AlN and AlN–O as in the case of crystalline sapphire. Such scenario also explains easier nitrogen uptake by $a\text{-Al}_x\text{O}_y$ buffers on Al_2O_3 substrate. Then the substrate acts as an additional reservoir of oxygen, so creation of O vacancies required for nitrogen diffusion and formation of AlN and AlN–O phases is much less efficient than in $a\text{-Al}_x\text{O}_y$ films on Si substrates.

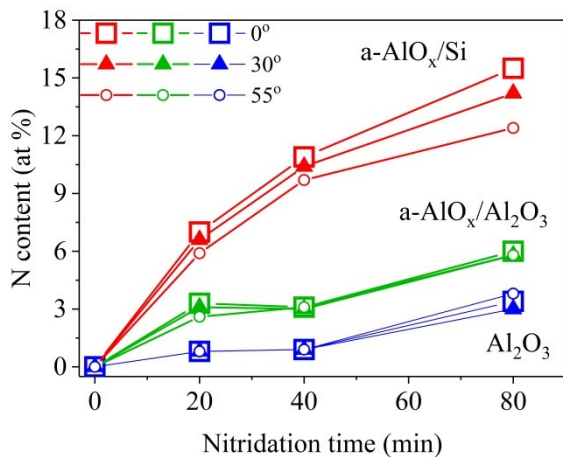


Fig. 5. The content of incorporated N as a function of nitridation time measured at 0° , 30° and 55° angles in respect to the surface normal for $a\text{-AlO}_x$ buffer layers on Si (red symbols) and sapphire (green symbols) substrates, and for bare crystalline sapphire (navy symbols). Squares denote 0° , triangles 30° , and circles 55° incident angles. Figure from [H2].

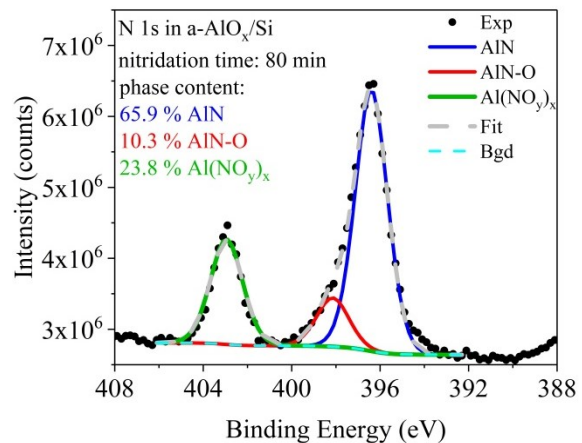


Fig. 6. The deconvoluted N 1s XPS line for $a\text{-Al}_x\text{O}_y/\text{Si}$ sample nitridated for 80 min at 800°C . Figure from [H2].

XPS results presented in [H2] indicate that the local $\text{Al}(\text{NO}_y)_x$ phase inclusions appearing on surface of $a\text{-Al}_x\text{O}_y$ buffer during the NW incubation period might play the role of heterogeneous nucleation centers responsible for efficient GaN NW formation on such buffers. Then, their absence in nitridated crystalline substrates would explain problems with NW growth on such substrates under our growth conditions. However, we do not treat that finding as the final answer of the question on the nature of centers inducing GaN nucleation

on such substrates. They are rather an indication for further studies. For example, numerical simulations of GaN crystallization and comparison of GaN formation energy on surfaces of all three phases detected in XPS experiments would be important for judging which from those three phases would be energetically the most favorable for GaN growth.

We have used the effect of efficient formation of GaN NWs on a- Al_xO_y buffers for selective area growth (SAG), i.e. for positioning the NWs in precisely defined areas on the substrate. This topic has been discussed in our two papers [H3] and [H4]. The first one is devoted to study of NW growth on GaN/sapphire substrates with narrow a- Al_xO_y nucleation stripes.

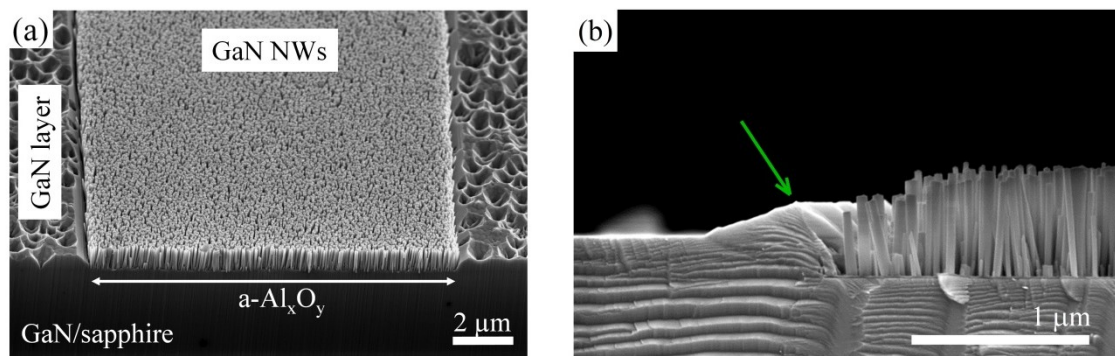


Fig. 7. SEM images of surface (a) and cross-section (b) of GaN grown on GaN/sapphire substrate with 12 μm wide a- Al_xO_y nucleation stripe. The green arrow in (b) marks enhanced edge GaN planar growth. Figure from [H3].

Figure 7 shows that GaN growth on such substrate led to crystallization of NW array on the a- Al_xO_y stripe while on the rest of the substrate a rough compact GaN layer with surface morphology typical for growth under N-rich conditions was formed. Obviously our priority was the NW growth, so the question arose if by making use of different mechanisms of planar and NW growths the conditions could be adjusted to maximize the height of NWs h while the thickness of compact layer d is minimized? In other words, could the Ga (Φ_{Ga}) and N (Φ_{N}) fluxes be adjusted to maximize the value of the aspect ratio $AR = h/d$? In the analysis performed we assumed that under N-rich conditions thickness of the compact layer was the product of the Ga flux and the growth time $d = \Phi_{\text{Ga}} \times t$. For nanowires situation was different and despite the overall N-rich conditions, due to Ga diffusion along the NWs' sidewalls to the top facets, NWs could grow Ga-rich [25]. Then the NW growth rate was limited by the N-flux and its height could be described as $h = \Phi_{\text{N}} \times (t - t_1)$, where the delay of NW nucleation onset t_1 was included. As the result, the aspect ratio AR could be calculated from the following equation:

$$AR = h/d = \frac{\Phi_N \times (t - t_1)}{\Phi_{Ga} \times t}, \quad (3)$$

where Φ_{Ga} and Φ_N are Ga and N fluxes, respectively, t is the growth time and t_1 the NW incubation time described by equation (2). Fig. 8 shows dependence of AR value on Ga and N fluxes calculated from Eqs. (2) and (3) for the growth temperature of 814°C and growth time of 120 min. The map is a convenient tool for controlling the aspect ratio for various growth conditions. In particular, it shows that for a fixed Ga flux the AR value fast increases with the impinging N flux. This is due to faster N-limited growth of NWs as well as to their shorter incubation period [H1]. For a fixed N flux larger AR values are expected for smaller Ga fluxes since this corresponds to thinner compact layer grown under Ga-limited conditions. These predictions were verified experimentally by growing GaN structures for various Φ_{Ga} and Φ_N values. The results are marked with stars in Fig. 8 where labels of experimental points give values of the AR parameters measured by SEM on cross-sections of respective samples. Excellent agreement of calculations and experiment is found for points marked in green. If however, the nitrogen flux is too large, or the Ga flux is too small Eq. (3) predicts AR values much larger than those measured experimentally. Such discrepancy shows that for too large N flux (or too small Ga flux) gallium adatom diffusion along sidewalls to the NW top facet is not efficient enough to create Ga-rich conditions there. In other words, for samples marked in red in Fig. 8 their growth conditions are not correctly described by Eq. (3) that assumes NW growth limited by nitrogen, i.e. faster than observed experimentally.

Fig. 7b shows enhanced growth of the compact GaN layer (marked with the arrow) in the vicinity of the a-Al_xO_y stripe. Simultaneously, GaN NWs close to the other side of the edge are shorter than in the middle of the stripe. We have explained faster edge growth of planar GaN as being due to surface Ga diffusion from the stripe during the incubation stage of NW formation. As long as there are no GaN nuclei formed on the stripe surface Ga concentration there is high because desorption is the only way of Ga consumption. Once crystallization of compact GaN begins the Ga diffusion from the stripe through the boundary starts. Since compact layer growth takes place under N-rich conditions an additional diffusional flux of Ga from the a-Al_xO_y covered part of the substrate increases planar growth rate close to the boundary leading to the excess edge growth. At the same time gallium out diffusion reduces Ga adatom concentration on the other side of the boundary leading to locally longer incubation time and shorter NWs there. Profile of NWs' height distribution at the edge of the

stripe (see Fig. 7b) allowed us to estimate the Ga diffusion length on $a\text{-Al}_x\text{O}_y$ as ~ 500 nm under our growth conditions.

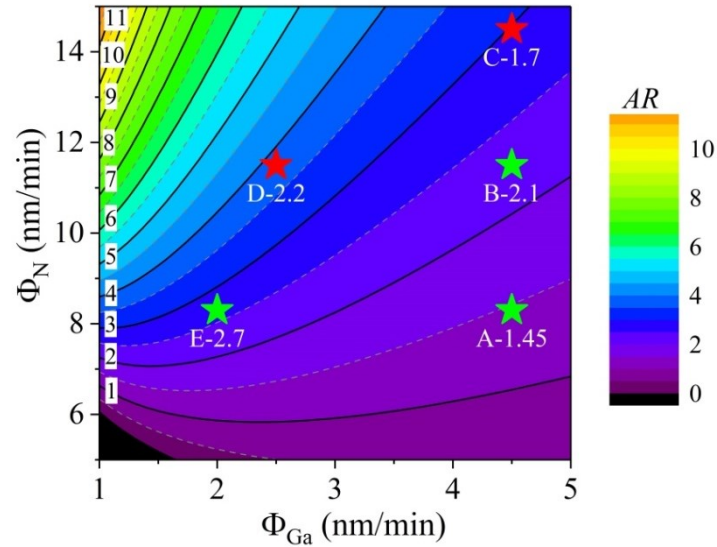


Fig. 8. Contour plot of the value of the aspect ratio AR as a function of nitrogen Φ_N and gallium Φ_{Ga} fluxes calculated from equation (3) for the growth temperature of 814°C and growth duration t of 120 min. Stars mark growth conditions for samples A–E while the labels give experimental values of the aspect ratio measured for these samples. Figure from [H3].

The results presented above show again that $a\text{-Al}_x\text{O}_y$ buffer is an efficient nucleation layer for GaN nanowires. Experiments performed allowed determination of the growth conditions under which the NWs grow Ga-rich despite external N-rich conditions. Also the origin of excess edge growth of compact GaN was clarified together with estimation of Ga adatom diffusion length on $a\text{-Al}_x\text{O}_y$ surface. However, the obtained values of the aspect ratio AR are quite small and for practical application formation of NWs outside the nucleation stripe should be avoided to achieve a full growth selectivity.

Example of such solution is presented in [H4] where surface diffusion of Ga adatoms is discussed as a source of spatial nonuniformity of GaN NWs grown by SAG. The growth was performed on Si substrates with narrow $a\text{-Al}_x\text{O}_y$ nucleation stripes while the rest of the substrate was covered by a thin silicon oxide mask. As we have shown in [H1], under the same conditions the NW incubation time on SiN_x/Si substrates is several times longer than on $a\text{-Al}_x\text{O}_y$. Thus the growth conditions can be found under which GaN NWs form exclusively on the nucleation stripes while nucleation on the mask surface is prohibited. Fig. 9 shows that in our case a full growth selectivity has been successfully achieved.

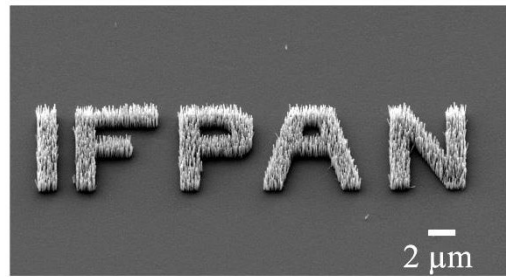


Fig. 9. Selective area growth of GaN NWs on a-Al_xO_y nucleation layer with SiN_x mask. Figure from [H4].

When analyzing the NW height distribution across the nucleation stripe we noticed that the NWs in the vicinity of the stripe edge are longer than those in the middle, which is the opposite behavior to that observed in [H3]. The effect is illustrated in Fig. 10b that shows the NW height distribution measured across the a-Al_xO_y nucleation stripe. Moreover, the nonuniformity of NW height strongly depended on the width of the stripe: for the NWs at the stripe's edge their height was nearly unchanged even for the narrowest stripes (blue points on Fig. 11). However, the height of NWs located in the middle of the stripe (green points) increased rapidly up to their length at the edge when the stripe width became smaller than $\sim 1 \mu\text{m}$.

We have considered various mechanisms that could lead to faster NW growth in vicinity of the edge of the nucleation layer: for example, the effect that Ga desorbing from the mask is captured by growing NWs as it was observed during MBE growth of GaP NWs [29]. If GaN NWs were grown under N-rich conditions this might indeed locally lead to their faster growth. However, our measurements showed that *during the elongation period* the NW growth rate was limited by nitrogen, not by gallium flux. Moreover, the NWs were quite dense and probability that Ga desorbing from the mask affects NW growth so far inside the stripe is low due to shadowing effect. It is noticing worthy however, that as shown in Fig. 11 the NW height nonuniformity disappears when width of the stripe reduces below $\sim 1 \mu\text{m}$, which is double the diffusion length of Ga on a-Al_xO_y [H3] and thus suggests a diffusional nature of the effect.

In order to clarify when the spatial nonuniformity of GaN NWs starts the growth was stopped just after the incubation time calculated from Eq. (2). Then distributions of density and size of GaN nuclei on the substrate were measured.

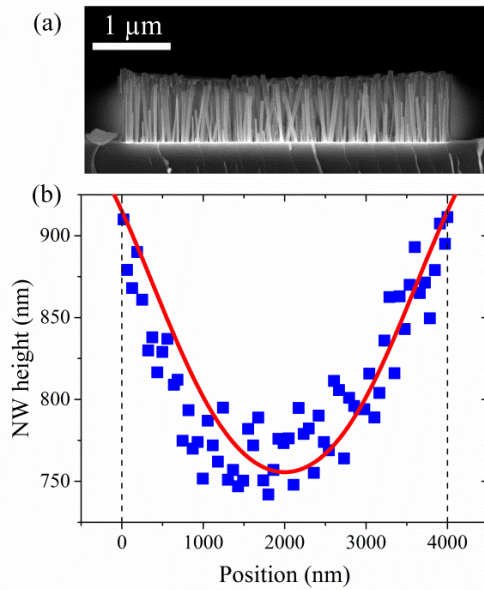


Fig. 10. Cross-section SEM image of ensemble of GaN NWs grown in 4 μm wide $\text{a-Al}_x\text{O}_y$ stripe after 120 min of growth. (b) Respective NW height distribution measured across the stripe. The line in (b) shows the height profile fitted by the model as described in the theoretical section. Figure from [H4].

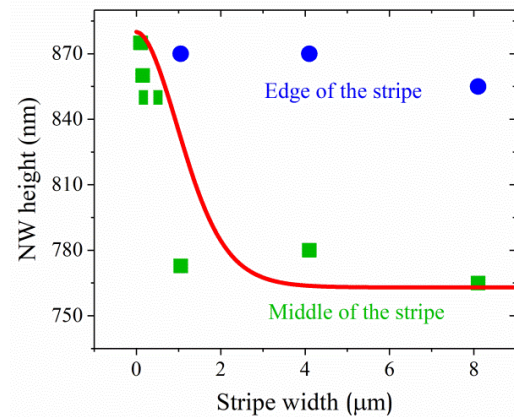


Fig. 11. (a) Average NW height at the edge (blue symbols) and in the middle (green symbols) of the stripe as a function of the stripe width. The red line shows the NW height in the middle of the stripe fitted by the model. Figure from [H4].

Fig. 12a presents top view SEM image of GaN nuclei formed during so short growth process while lower panels show distributions of nuclei density (b) and their average size (c) across the $\text{a-Al}_x\text{O}_y$. As seen, at the very beginning of the nucleation period the GaN nuclei are larger and more dense at the edge than in the middle of the stripe. This means that nonuniformity of NWs appears at their early nucleation stage already. However, in this case, on the contrary to the previous one illustrated in Fig. 7, diffusional exchange of Ga adatoms with the outside of the nucleation stripe *during incubation of NWs* is impossible since there are no GaN crystallites there that could consume gallium. Moreover, as discussed in detail in [H4], a shorter lifetime of Ga adatoms and thus their lower concentration are expected on the SiN_x mask surface whereas eventual Ga surface diffusion from the nucleation $\text{a-Al}_x\text{O}_y$ stripe, if any, should be blocked by the Ehrlich-Schwöebel barrier at the high mask edge.

Our considerations have led to the scenario in which surface diffusion of Ga adatoms from the mask into the nucleation stripe starts at the beginning of the NW *nucleation stage*. The first GaN nuclei appearing on the surface capture extra Ga adatoms from the mask, grow faster and are more dense than in the middle of the stripe. Consequently, the NWs in the vicinity of the stripe edge are longer than in its middle. Obviously, diffusion induced

nonuniformity of nuclei size and density, and in turn height of NWs, strongly decreases when the mask delivers extra Ga adatoms to the whole nucleation stripe, i.e. when its width is less or equal to the double Ga diffusion length on a-Al_xO_y. This is exactly the behavior shown in Fig. 11.

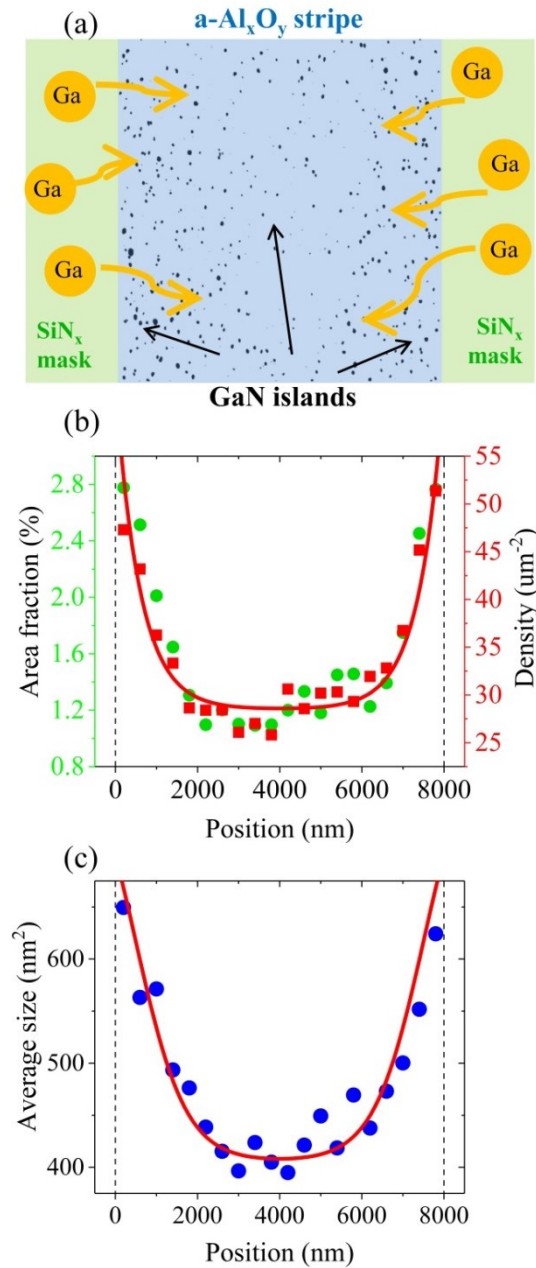


Fig. 12. SEM image of GaN nuclei (a) and distributions of their density (b) and average size (c) across the a-Al_xO_y nucleation stripe. Full lines show results of calculations. Yellow arrows in (a) schematically show direction of Ga surface diffusion from the mask into the stripe at the nucleation stage of NW formation. Figure from [H4].

In cooperation with theoreticians from the group headed by prof. Vladimir Dubrovskii from St. Petersburg State University a model has been developed that describes influence of surface Ga diffusion from the SiN_x mask into a-Al_xO_y nucleation stripe on nucleation and

growth of GaN NWs. Results of calculations are shown as full lines in Figs. 10 – 12. Excellent agreement has been obtained for Ga diffusion length on $a\text{-Al}_x\text{O}_y$ equal to 600 nm, i.e. close to our earlier predictions [H3]. Finally, I want to emphasize that results of our analysis are not limited to our growth system only. On a general note, our findings demonstrate that due to significance of diffusive mass exchange between various parts on substrate the nucleation and growth kinetics in selective area growth depends on the size of the pattern, which makes it very different from growth on the equivalent planar layers.

As I mentioned already, we showed in our earlier work [B27] that on SiN_x/Si substrate the rate of spontaneous GaN nucleation is limited by surface concentration and diffusion rate of Ga adatoms. This is true, however, only if surface of Si substrate is clean, so the SiN_x layer formed during substrate nitridation in MBE growth chamber is continuous and perfectly uniform. Residual surface contaminations disturb the nitridation process which can lead to a local change of the nucleation mechanism and consequently to modification of parameters of NWs. In particular, it is well known that self-induced GaN NWs grown by PAMBE on nitridated Si substrate should have the nitrogen polarity (N-polar) [B16]. Quite often, however, a mixed polarity, i.e. presence of NWs of different polarities inside one sample, is reported [30, 31] while the origin of the effect has not been clarified yet.

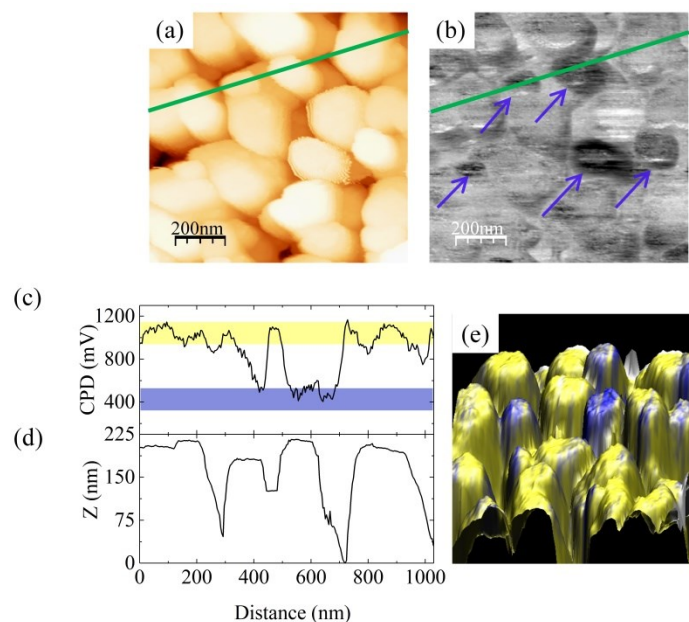


Fig. 13. (a) AFM topographic view image ($1 \times 1 \mu\text{m}^2$) and (b) the corresponding contact potential difference (CPD) map (color scale from 0 to 1.5 V) of GaN NW array grown on HF-etched Si substrate. Violet arrows in (b) mark Ga-polar NWs. The CPD value and NW height profiles along the green line, (c) and (d), respectively. (e) shows the 3D superposition of the topography (xyz axis) and CPD value (color scale). Violet marks Ga-polar and yellow N-polar NWs. Figure from [H5].

In the work [H5] Kelvin Probe Force Microscopy (KPFM) was used to study uniformity of GaN NWs grown on nitridated Si(111) substrates. KPFM technique is based on the local measurement of the contact potential difference (CPD) between the NW top facet and the atomic force microscopy (AFM) tip, which is known to depend strongly on GaN polarity [31]. By contrast to the techniques based on electron microscopy, KPFM is nondestructive and allows the polarity assessment of a statistically significant number of single NWs over micrometer large surface areas with nanometer resolution and without the need of any special sample preparation [32]. Particularly interesting for us was an influence of Si substrate cleaning procedure, so potentially its cleanness, on uniformity of polarity in an ensemble of GaN NWs. As example, Fig. 13 presents AFM (a) and CPD value (b) maps of the same area of the NW array. The substrate for this growth process was dipped in diluted HF solution and then transferred in air to the load lock chamber of the MBE system. As it is well known, etching of silicon in diluted HF removes surface oxides and leaves the surface passivated by absorbed hydrogen which is expected to protect the wafer against oxidation [33 – 35]. In the next step hydrogen passivation is removed by UHV annealing in the growth chamber at $\sim 700^\circ\text{C}$. This results in appearance of the 7×7 surface reconstruction on the RHEED pattern that is commonly accepted as a fingerprint of a clean Si(111) surface. Due to a simplicity of such procedure the HF dipping is the most common way of Si substrate preparation prior to GaN NW growth [36 – 40]. However, our results presented in Fig. 13 show that many of NWs analyzed in the sample ($\sim 18\%$ from 125 NWs tested) exhibit unexpected gallium polarity. Similar effect of mixed polarity has been reported already for NW growth of HF-treated Si substrates [30, 31]. As will be explained in detail below, presence of Ga-polar NWs can be correlated with residual oxide islands left on the substrate, so indicates limited efficiency of hydrogen passivation protection of the surface against oxidation. In the work [H5] many other alternative protocols of Si substrate preparation for GaN NW growth (RCA etching, deoxidation in Ga flux, etc.) were tested. However, complete elimination of mixed polarity was obtained only after thermal removal of native silicon oxide at $\sim 1000^\circ\text{C}$ under UHV conditions. This requires, however, that the growth system is equipped with a high temperature substrate heater, which not always is the case. This partly explains why the more easy HF treatment procedure is so commonly used.

Importantly, similar effect of uniform N polarity with a certainty above 99.8% (more than 400 NWs tested) was found for GaN NWs grown on Si substrate with $a\text{-Al}_x\text{O}_y$ buffer (Fig. 14), despite the fact that Si was first HF-treated and then exposed to air for more than 1 hour before buffer deposition. This shows that $a\text{-Al}_x\text{O}_y$ buffer efficiently buries residual oxides and

provides uniform and clean surface for NW growth. On a general note, our findings demonstrate that presence of 7×7 surface reconstruction in RHEED pattern is not a proof of absolute surface purity, especially if the RHEED pattern is treated qualitatively only without precise quantitative analysis. In that sense, appearance of the NWs with inverted polarity is much more sensitive indicator of local substrate contamination. The problem is, however, that on Si(111) substrate both types of NWs are perpendicular to the substrate and cannot be easily distinguished by simple techniques, as for example SEM. Much more complicated techniques as KPFM must be used to detect local polarity inversion of NW.

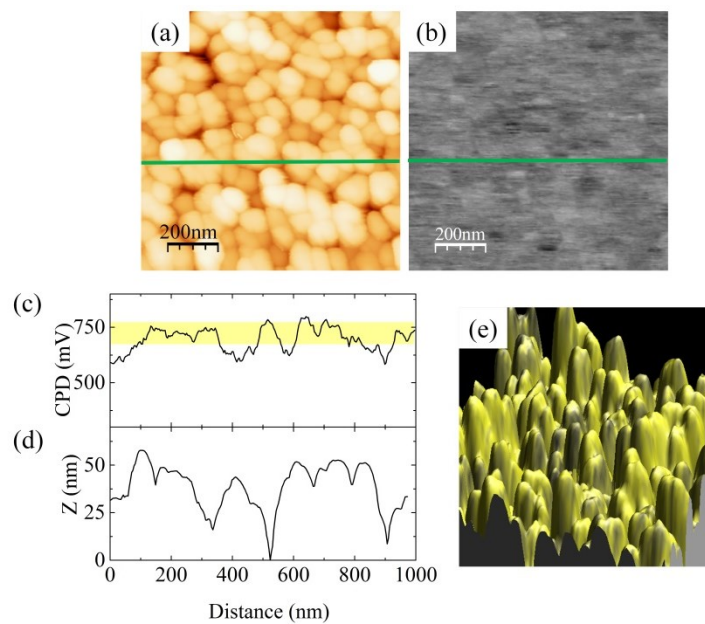


Fig. 14. (a) AFM topographic view image ($1 \times 1 \mu\text{m}^2$) and (b) the corresponding CPD map (color scale from 0 to 1.5 V) of GaN NW array grown a- Al_xO_y . The CPD value and NW height profiles along the green line, (c) and (d), respectively. (e) shows the 3D superposition of the topography (xyz axis) and CPD value (color scale). Figure from [H5].

As we have shown in our work [H6] situation is different if Si substrate has (001) orientation. Then, depending on the procedure used for substrate preparation SEM images show two types of GaN NWs: perpendicular and inclined at the angle of $\sim 60^\circ$ to the substrate (Fig. 15). Studies by laboratory X-ray diffraction did not show any differences of both NW systems except different orientation of the c axis of GaN. However, when Grazing Incidence X-Ray Diffraction (GIXRD) employing intense synchrotron X-ray source was applied then additional reflections from cubic GaN were detected in the sample with inclined NWs (Fig. 16).

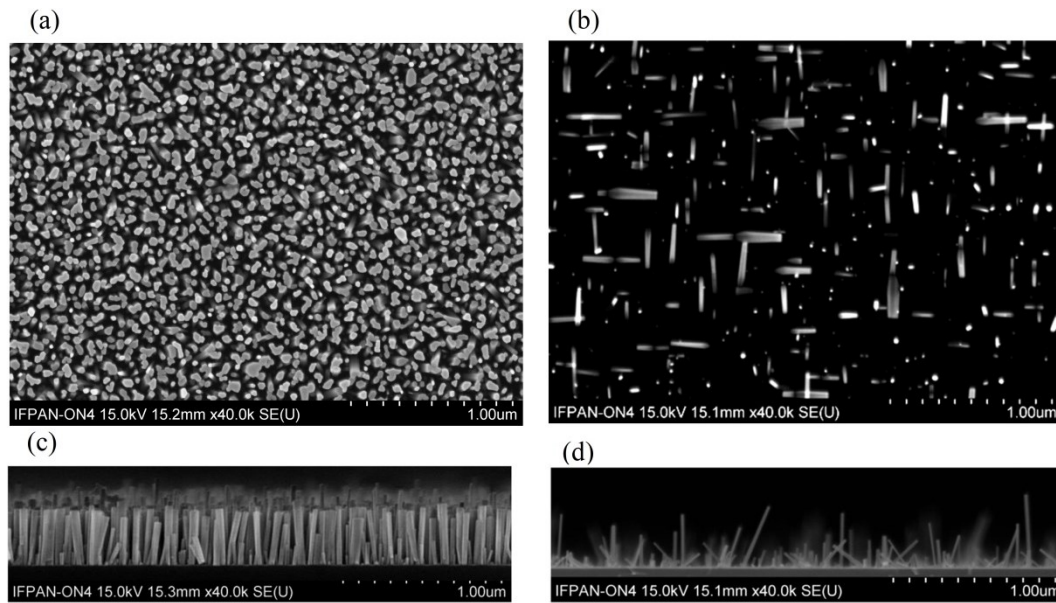


Fig. 15. Top view (a)–(b) and cross-section (c)–(d) SEM micrographs of GaN NW *Sample 1* and *Sample 2* in the left and the right column, respectively. Figure from [H6].

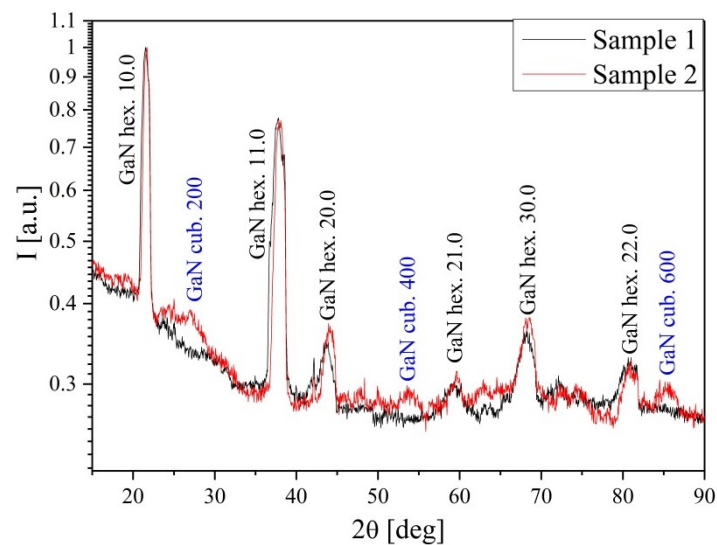


Fig. 16. GIXRD scans for perpendicular NWs (*Sample 1*) and for mostly inclined nanowires (*Sample 2*) to Si(001) substrate. Figure from [H6].

The zb-GaN parts are shown at the boundary of NWs with the substrate in TEM images collected in Fig. 17. The NWs in *Sample 1* nucleated and then grew perpendicular to the substrate in wurtzite structure on top of the SiN_x layer formed during substrate nitridation. The *Sample 2* contained another type of NWs oriented perpendicular to the Si(111) planes and thus inclined to the substrate surface (Fig. 17). As shown in Fig. 17b they formed directly on the silicon surface, i.e. without intermediate SiN_x film, initially as zb-GaN islands. Next, their sidewalls transformed into more stable hexagonal phase and inclined wurtzite GaN NWs grew

having Ga polarity. We have correlated formation of inclined NWs with presence of island of residual silicon oxide left on the substrate after the HF etch, as explained in the work [H5]. Those islands act as a mask locally blocking formation of the SiN_x film during substrate nitridation. When the growth starts these islands are dissolved in Ga flux, Ga-assisted nucleation of GaN proceeds from Ga droplets located in discontinuities in the SiN_x film and finally inclined NWs are formed in a direct contact the silicon substrate. We have verified that this scenario by using HF-treated Si(001) substrate that was initially nitridated, then cleaned in Ga flux and nitridated again to fill in the oxide-induced voids in the SiN_x film. Growth of GaN NWs on so prepared substrate led to formation of the NWs perpendicular to the substrate while no inclined NWs were obtained (*Sample 1*).

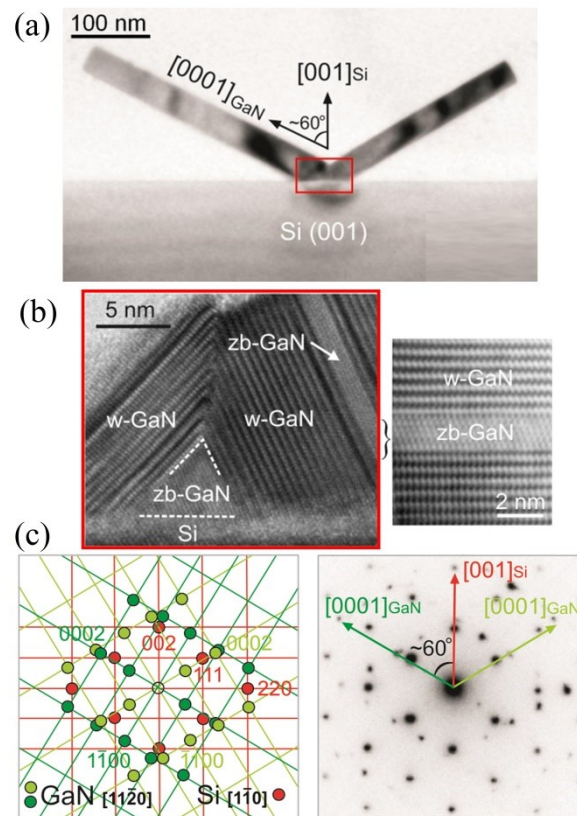


Fig. 17. Cross-sectional TEM image of inclined (a) GaN NWs in *Sample 2*; (b) HRTEM image of the zoomed area of the interface between the inclined NW and the Si substrate; (c) diffraction image of the NW pair with Miller indices of the lattice planes. Figure from [H6].

Our findings show a crucial role of silicon nitride interlayer for growth mode and crystallographic alignment of GaN nanowires on silicon substrate. Moreover, we found a direct correlation of presence of both types of NWs with the procedure used for preparation

of Si substrate for GaN epitaxy, which in connection to the work [H5] offers a way to induce or block formation of nanowires of the required type.

4.4. Main achievements – summary

The main achievements presented in the series of publications [H1] – [H6] are:

- a comprehensive analysis of the kinetics of spontaneous nucleation of GaN nanowires and analytical description of the dependence of their incubation time on the parameters of the PAMBE growth process, which enabled:
 - ❖ calculation of maps illustrating the values of GaN incubation times under conditions not explored experimentally; application of these maps for development of efficient methods of controlling the GaN incubation stage by selecting the crystallization conditions and the substrate (a-Al_xO_y vs. SiN_x) [H1],
 - ❖ modeling and experimental verification of the growth diagram showing the range of growth parameters favoring formation of GaN nanowires or planar GaN layer on a-Al_xO_y [H1],
 - ❖ demonstrating that a-Al_xO_y is much more efficient nucleation layer for GaN nanowires than the commonly used SiN_x/Si substrate, offering shorter incubation times and a much wider range of growth parameters enabling formation of nanowires [H1],
 - ❖ development of a technology for selective area formation of GaN nanowires on GaN [H3] and SiN_x/Si [H4] substrates with a-Al_xO_y nucleation layer,
 - ❖ determination, by comparison of experimental results with calculations, of the range of growth conditions under which, due to Ga diffusion along the sidewalls to upper surfaces, GaN NWs crystallize under local gallium rich conditions despite an external nitrogen excess [H3];
- development of a model that quantitatively describes the surface diffusion of Ga adatoms during the selective area growth of GaN NWs and its application to explain the spatial nonuniformity of nanowires; determination of the diffusion length of Ga adatoms on the a-Al_xO_y surface by adjusting the model predictions to the experimental data [H4];

- showing that during the selective area formation of nanowires on the GaN/sapphire substrate an excess planar edge growth as well as the smaller length of nanowires at the edge of the nucleation stripe, result from the surface Ga mass transport from a-Al_xO_y stripe towards GaN layer during the incubation period of nanowires [H3];
- identification of residual oxide islands as a source of the mixed polarity effect and modification of crystallographic arrangement of GaN nanowires on Si substrates; demonstration that a-Al_xO_y buffer layer efficiently buries residual silicon oxides on Si substrate providing a clean and stable surface for the PAMBE growth of nanowires with uniform nitrogen polarity and well-ordered orientation perpendicular to the substrate surface [H5] and [H6];
- proposing a mechanism of nitrogen incorporation into a-Al_xO_y/Si and a-Al_xO_y/sapphire buffer layers during their annealing in nitrogen plasma under conditions imitating the incubation of GaN nanowires; indication that precipitations of the Al(NO_y)_x phase formed on the surface of the buffer during the incubation of nanowires may play a role of the local centers accelerating heterogeneous GaN nucleation on amorphous a-Al_xO_y buffers layers. Consequently, their absence in nitridated crystalline sapphire substrates explains the problems with forming nanowires on such substrates under our technological conditions [H2].

4.5. An importance of publications [H1] - [H6] for the development of GaN nanowires growth technology

In my opinion, the results obtained as a part of the habilitation achievement have significantly deepened our understanding of the physical phenomena occurring in the nano-scale during spontaneous GaN nucleation on non-crystalline substrates. However, apart from their importance for basic research in solid state physics, these results significantly contributed to the progress of our works on application of GaN nanowires structures. Understanding nucleation and growth mechanisms of GaN nanowires, so the processes described in the publications included to the presented scientific achievement, is crucial for the design and controlled crystallization of nanostructures with properties required for specific research applications.

For example, effective use of GaN nanowires in hybrid solar cells GaN – polymer P3HT:PC71BM requires the use of short (<100 nm) nanowires of equal lengths. This

requirement, being consequence of high absorption of light and its low penetration depth in the polymer, is generally quite difficult to meet during growth in the self-assembly mode, due to extended process of nucleation. The use of the results of our work on kinetics of nucleation and growth of NWs allowed crystallization of such structures by adjusting growth conditions in the way as to ensure very fast incubation and nucleation while keeping sufficiently slow growth of nanowires [A6, A8]. On the other hand, for spectroscopic studies of graphene transferred onto GaN NW array, long nanowires with large height dispersion and different Al contents in AlGaIn axial segments were needed. The aim was to control deformation and electrical properties of graphene by changing the average distance, diameter and chemical composition of its NW supports [A1, A4, A11]. Similarly, the analysis of the nucleation processes of GaN nanowires on various buffer layers presented in [H1] was of key importance for development of the technique of selective area formation of nanowires ([H3, H4]). Knowing the dependence of the incubation rate of GaN on the choice of substrate allowed to adjust the growth conditions so that nanowires grew only on nucleation layer, while GaN crystallization on the mask was blocked.

Our finding that regardless of the substrate, the self-assembled formation of nanowires by PAMBE technique proceeds in a similar manner (i.e. in the sequence of incubation, nucleation and elongation stages), allowed us to develop a technology of GaN NWs fabrication on metallic buffer layers (ZrN). As we have shown, the GaN/ZrN electrical contact shows a linear I-V characteristics. Thus, ZrN layer not only induces formation of nanowires, but simultaneously can play a role of buried contact with a high electrical conductivity to their bottom parts and act as a buried mirror efficiently reflecting visible light, which is particularly important e.g. in photodetector or LED structures. This solution has been patented by us [P1]. It opens the way to the construction of new devices based on GaN nanowires. For example, the application of ZrN nucleation layer is a very promising alternative to LED structures for which complicated growth of GaN nanowires on graphene layers is used [7]. In addition, the transfer of the NW ensemble grown on ZrN buffer from the host substrate to another flexible substrate (e.g. plastic or copper foils) becomes possible. This solution is well in line with recent intensive research on designing and fabrication of flexible electronic devices [41].

Similarly, our results on the selective area growth of GaN nanowires on $a\text{-Al}_x\text{O}_y$ buffers has got the national patent protection [P2]. As mentioned earlier, the significance of publications [H3, H4] is not limited to our specific growth configuration. They report a general phenomenon that due to adatom surface diffusion, kinetics of selective area

nucleation and growth of nanowires strongly depend on the size of the mask pattern and significantly differ from those observed during crystallization under the same conditions on homogeneous planar substrates. Currently, I am focusing on combining the results of our previous experiments and developing SAG of GaN nanowires with the use of metallic ZrN nucleation layers. I expect that this will lead to new designs of semiconductor devices based on group III nitride nanowires.

As very important I consider our findings reported in publications [H5, H6]. They show the fundamental role of the buffer layer, its homogeneity and a potential presence of residual impurities for the growth mechanism, crystallographic arrangement and electron properties of GaN nanowires. In particular, they shed new light on the origin of the mixed polarity effect which is often reported in nanowire assemblies. By showing a strong correlation of nanowires polarity with the process of Si substrate preparation for GaN crystallization, we indicated the possibility of blocking or inducing the formation of the desired type of nanowires. This has important practical implications since, as we have recently shown, the change of polarity strongly affects the electroluminescence efficiency of GaN/AlGaN nanowire structures with a p-n junction [A10].

5. Presentation of significant scientific or artistic activity carried out at more than one university, scientific or cultural institution, especially at foreign institutions

A significant part of my professional activity was carried out in cooperation with researchers from domestic and foreign scientific institutions established during conference meetings or my research stays at these centers. This significantly expanded my horizons enabling access to new research methods, both theoretical and experimental, as well as to the equipment unavailable at the Institute of Physics PAS. Below is the list of these centers and a short description of results of common works:

- **Paul-Drude-Institut für Festkörperelektronik, Berlin, Germany**

dr. Lutz Geelhaar and dr. Sergio Fernández-Garrido

Four research stays in Berlin to conduct research on nucleation and growth of GaN nanowires on a-Al_xO_y substrates by QMS technique. The results were published in [H1, B26] and in several joint conference presentations.

- **St. Petersburg University, St. Petersburg, Russia**

prof. Vladimir Dubrovskii

Modeling of nucleation of GaN nanowires on a-Al_xO_y and SiN_x buffer layers and Ga surface diffusion during selective area growth of GaN nanowires. The results were published in [H4, B27] and in the form of joint conference presentations.

- **University of Valencia, Valencia, Spain**

dr. Ana Cross

The use of Kelvin Probe Force Microscopy to analyze polarity of GaN nanowires grown on Si substrates. The results were published in [H5] and as joint conference presentations.

- **University of Arkansas, Fayetteville, USA**

dr. A. V. Kuchuk and dr. Yu. I. Mazur

X-ray diffraction measurements and modeling of strain in LED structures based on GaN/AlGaIn nanowires. The results were published in [A5, B23].

- **V. Lashkaryov Institute of Semiconductor Physics, NAS of Ukraine**

prof. Vasyl Kladko and dr. A. V. Kuchuk

One-week stay in Kiev to start cooperation on modeling of strain and X-ray diffraction curves of GaN/AlGaIn nanowires. The continuation of these common studies has led to the publications [B14, B20].

- **Ioffe Physical-Technical Institute, St. Petersburg, Russia**

dr. Dmitrii V. Nechaev

Optimization of PAMBE growth of planar AlN and AlGaIn layers on sapphire substrates. The results were published in [A9].

- **Institut für Angewandte Physik, Technische Universität Dresden, Dresden, Germany**

dr. Vladimir Kolkovsky

Investigation of electron properties of planar GaN and AlGaIn layers and GaN nanowire structures by deep level transient spectroscopy (DLTS). The results were published in [B5, B12, B21].

Simultaneously, I conducted joint research with many national universities and research centers:

- **Institute of Electron Technology in Warsaw (currently Łukasiewicz Network – Institute of Microelectronics and Photonics)**

In collaboration with *dr. Marek Ekielski*, we conducted research on the selective area formation of GaN nanowires. The results were published in [H3, H4] and presented during conference presentations.

- **Faculty of Physics, University of Warsaw**

In cooperation with *prof. Krzysztof Korona* optical properties of GaN and AlGaN nanowires and GaN/AlGaN heterostructures were studied. The results were presented in [A2, A6, A8, A10, B6, B16, B17, B21, B22] and in many conference presentations.

With *dr. Aneta Drabińska* and her coworkers, we conducted joint research on the properties of graphene layers deposited on GaN and AlGaN nanowires. The results were published in [A1, A4, A11].

- **Wroclaw University of Science and Technology**

In collaboration with *prof. Robert Kudrawiec* and *dr. Łukasz Janicki* from the Faculty of Semiconductor Materials Engineering, we carried out measurements of internal electric fields in GaN/AlGaN/GaN heterostructures and position of the Fermi level in planar air/GaN and graphene/GaN systems. The results were published in [A7, B10, B24, B28].

With *prof. Ewa Płaczek-Popko* and *dr. Eunika Zielony* from the Faculty of Physics, we conducted an analysis of electronic states in GaN nanowires and Raman studies of crystal lattice vibrations in GaN/AlGaN nanowires. The results were published in [B8, B9].

6. Presentation of teaching and organizational achievements as well as achievements in popularization of science

During my professional activity at the Institute of Physics PAS, I participated in teaching of students. In 2012, I conducted classes in the MBE ON4 laboratory with third and fourth year students of the Faculty of Mathematics and Natural Sciences at the Cardinal Stefan Wyszyński University in Warszawa. During the period of August 18 – September 11, 2015, I took care of two students from the Gdańsk University of Technology who completed their undergraduate training in our laboratory. Similarly, in 2018, another student from the Gdańsk University of Technology was undergoing an internship in the MBE ON4 laboratory under my supervision. Currently, I am a supervisor of two students from the Warsaw University of Technology preparing their master's theses in our laboratory. From November 2019 to October 2021, I was also an auxiliary supervisor of the PhD student Waqas Perwez who was working on his doctoral thesis at the Warsaw Doctoral School of Natural and BioMedical Sciences.

As for my organizational activities for the scientific community, I was a member of the Organizing Committee of the 17th International Conference on Crystal Growth and Epitaxy organized in August 2013 in Warszawa under auspices of the International Organization for Crystal Growth. I was responsible for editing of more than 900 abstracts submitted to the conference and the preparation for press of the Scientific Program and the Book of Abstracts (ISBN 83-89585-36-7) of the ICCGE 17 conference.

In order to contribute to a popularization of science, I prepared an invited review article presenting the activity of our group in the field of crystallization of nitride semiconductor nanostructures by PAMBE technique:

[B25] **M. Sobańska**, A. Wierzbicka, K. Kłosek, G. Tchutchulashvili, J. Borysiuk, Z.R. Żytkiewicz

Mechanizm spontanicznego zarodkowania i wzrostu techniką MBE oraz właściwości nanodrutów GaN (Mechanism of spontaneous nucleation and growth by MBE technique and properties of GaN nanowires)

Postępy Fizyki 67 (2016) 45–58

ISSN 0032-5430

[Postępy Fizyki 67 \(2016\) 45–58](#)

The paper was published in the special issue of *Postępy Fizyki* prepared on the occasion of the 100th anniversary of the discovery of the Czochralski growth method and contained a collection of articles presenting an overview of activities on crystal growth and properties of crystalline materials in Poland. In January 14 – 18, 2013, I participated in the workshop *Physics of Magnetism, Superconductivity and Semiconductors and Biophysics* for talented schoolchildren organized at the Institute of Physics PAS in cooperation with the National Children's Fund.

7. Description of scientific achievements unrelated to the topic of habilitation

As it was mentioned already, my main research activity is focused on physics and crystallization technology of group III nitride nanowires. However, participation in many other research projects (see point II.5 in Attachment No. 4) and scientific cooperations (see point 5 of Summary of Professional Accomplishments) caused my involvement in various research works not directly related to the topic of my habilitation.

A significant part of them is related to GaN and AlN planar layers and GaN/AlGaIn heterostructures dedicated to specific projects. For example, in the framework of the InTechFun project, I was working on growth technology of GaN layers on Si substrates [B7]. In particular, we showed that a direct PAMBE crystallization of GaN on Si unavoidably resulted in a local dissolution of silicon substrate in liquid gallium and a high concentration of surface defects. It was necessary to initiate the growth by deposition of a thin AlN layer on the substrate, which protected the substrate against reaction with gallium, and at the same time reduced the stress caused by different thermal expansion coefficients of Si and GaN. As a part of the NanoBiom project, we conducted research on PAMBE growth and characterization of AlGaIn/GaN HEMT transistor structures [B3, B10, B15]. This included structural characterization of GaN/AlGaIn structures [B3, B15], measurements of electron concentration distribution in such structures, as well as the analysis of AlN interlayer influence on distribution of electric fields in HEMT structures and concentration of carriers in their two-dimensional channels [B10].

Within the same project, we developed a method of controlling nitrogen flux delivered by a plasma nitrogen cell. For that we measured the light emission spectrum of the plasma in the cell cavity, which allowed to determine the intensity changes of the characteristic emission lines as a function of the nitrogen gas flow and the RF coil power [B11]. This led to the identification of the active state of nitrogen species emitted from the cell (atomic nitrogen vs. excited molecular nitrogen) as a function of the cell operational parameters. This is important

information because it is known that energy state of the nitrogen precursor affects the atomic processes active during GaN crystallization and possible creation of point defects in the crystal [42 – 44]. It also enables precise control of active nitrogen flux. Currently, this technique is routinely used in our laboratory to ensure high reproducibility of crystallization processes of planar structures, which are typically performed under nitrogen limited (i.e. gallium-rich) growth conditions.

I also participated in the project devoted to optical properties of GaN/AlGaN quantum wells [A3] and analysis of their structural quality [B4], as well as in projects on measurements of electrical properties of GaN and AlGaN layers [B5], as well as photoluminescence of AlN layers on sapphire substrates [A9]. I actively collaborated with the group of prof. Robert Kudrawiec from Wrocław University of Science and Technology by preparing epitaxial structures for measurements of electric field distribution in GaN/AlGaN/GaN heterostructures [B24] and position of the Fermi level at air/GaN [B28] and graphene/GaN [A7] interfaces. The examples above clearly show that protocols of planar growth of nitride semiconductors developed with my participation, enabled interesting studies of physical properties of such heterostructures.

Similarly, initiated and carried out by me, technological works related to the spontaneous nucleation and crystallization of GaN/AlGaN nanowires by PAMBE allowed studying specific properties of these objects. In particular, this includes studies of a nature of characteristic 3.42 eV luminescence of GaN nanowires (related to the recombination of excitons on stacking faults created during coalescence of nanowires) [B17], an influence of local strain on cathodoluminescence of GaN/AlGaN nanowires [B23], electron levels in overgrown GaN nanowires with a p-n junction analyzed by I-V and DLTS techniques [B12, B21] and crystal lattice vibrations in GaN nanowires observed by Raman spectroscopy [B8, B9]. After PhD defense I started cooperation with the group of dr. Aneta Drabińska from the University of Warsaw, who was interested in GaN and GaN/AlGaN NW arrays as a base onto which graphene was transferred. The results of these studies showed that an interaction with NWs resulted in a significant deformation of graphene layer, modification of its electrical properties and surface-enhanced Raman scattering effect. Results of these studies were published in [A1, A4, A11].

As recommended by the Council of Scientific Excellence my other achievements, including the list of lectures and conference presentations, patents, awards, participation

in research projects, organizational and teaching activities, and the values of scientometric parameters are presented in the Attachment No. 4.

8. References

As shown in the list of my publications (Attachment No. 4), publications included to the habilitation thesis were marked by the H letter, the letter A was used for articles published after PhD defense, and papers published before the defense were marked by B letter. The letter P points my patents (list in Attachment No. 4, point III.1).

- [1] K. Kishino, S. Ishizawa, *Nanotechnology* **26** (2015) 225602.
- [2] E.P.A.M. Bakkers, M.T. Borgstrom, M.A. Verheijen, *MRS Bull.* **32** (2007) 117.
- [3] S. Conesa-Boj, E. Russo-Averchi, A. Dalmau-Mallorqui, J. Trevino, E.F.Pecora, C. Forestiere, A. Handin, M. Ek, L. Zweifel, L.R. Wallenberg, D.Ruffer, M. Heiss, D. Troadec, L. Dal Negro, P. Caroff, A. Fontcuberta i Morral, *ACS Nano* **6** (2012) 10982.
- [4] A. Kikuchi, M. Kawai, M. Tada, K. Kishino, *Jpn. J. Appl. Phys.* **43** (2004) L1524.
- [5] H. Sekiguchi, K. Kishino, A. Kikuchi, *Electron. Lett.* **44** (2008) 151.
- [6] K. Kishino, J. Kamimura, K. Kamiyama, *Appl. Phys. Express* **5** (2012) 031001.
- [7] I.M. Høiaas, A.L. Mulyo, P.E. Vullum, D-C. Kim, L. Ahtapodov, B.O. Fimland, K. Kishino, H. Weman, *Nano Letters* **19** (3) (2019) 1649-1658.
- [8] K. Kishino, J. Kamimura, K. Kamiyama, *Appl. Phys. Express* **5** (2012) 031001.
- [9] J.C. Johnson, H.J. Choi, K.P. Knutsen, R.D. Schaller, P.D. Yang, R.J. Saykally, *Nature Mater.* **1** (2002) 106.
- [10] R.S. Chen, H.Y. Chen, C.Y. Lu, K.H. Chen, C.P. Chen, L.C. Chen, Y.J. Yang, *Appl. Phys. Lett.* **91** (2007) 223106.
- [11] L. Rigutti, M. Tchernycheva, A.D. Bugallo, G. Jacopin, F.H. Julien, L.F. Zagonel, K. March, O. Stephan, M. Kociak, R. Songmuang, *Nano Lett.* **10** (2010) 2939.
- [12] Q. Li, J.B. Wright, W.W. Chow, T.S. Luk, I. Brener, L.F. Lester, G.T. Wang, *Opt. Express* **20** (2012) 17873–17879.
- [13] B. Damiliano S. Vézian, J. Brault, B. Alloing, J. Massies, *Nano Lett.* **16** (2016) 1863 – 1868.

- [14] Q. Li, K.R. Westlake, M.H. Crawford, S.R. Lee, D.D. Koleske, J.J. Figiel, K.C. Cross, S. Fatholouloumi, Z. Mi, G.T. Wang, *Opt. Express* **19** (2011) 25528.
- [15] L. Geelhaar, C. Chèze, B. Jenichen, O. Brandt, C. Pfuller, S. Munch, R. Rothmund, S. Reitzenstein, A. Forchel, T. Kehagias, P. Komninou, G.P. Dimitrakopoulos, T. Karakostas, L. Lari, P.R. Chalker, M.H. Gass, H. Riechert, *IEEE J. Sel. Top. Quantum Electron.* **17** (2011) 878.
- [16] L. Lari, T. Walther, M.H. Gass, L. Geelhaar, C. Chèze, H. Riechert, T.J. Bullough, P.R. Chalker, *J. Cryst. Growth* **327** (2011) 27–34.
- [17] C. Chèze, L. Geelhaar, O. Brandt, W.M. Weber, H. Riechert, S. Munch, R. Rothmund, S. Reitzenstein, A. Forchel, T. Kehagias, P. Komninou, G.P. Dimitrakopoulos, T. Karakostas, *Nano Res.* **3** (2010) 528–536.
- [18] M. Yoshizawa, A. Kikuchi, M. Mori, N. Fujita, K. Kishino, *Jpn. J. Appl. Phys.* **36** (1997) L459.
- [19] M. Yoshizawa, A. Kikuchi, N. Fujita, K. Kushi, H. Sasamoto, K. Kishino, *J. Cryst. Growth* **189/190** (1998) 138.
- [20] M.A. Sánchez-García, E. Calleja, E. Monroy, F.J. Sánchez, F. Calle, E. Muñoz, R. Beresford, *J. Cryst. Growth* **183** (1998) 23.
- [21] E. Calleja, M.A. Sánchez-García, F.J. Sánchez, F. Calle, F.B. Naranjo, E. Muñoz, S.I. Molina, A.M. Sanchez, F.J. Pacheco, R. Garcia, *J. Cryst. Growth* **201/202** (1999) 296.
- [22] J.E. Northrup, J. Neugebauer, *Phys. Rev. B* **53** (1996) R10477.
- [23] B.Q.Y. Tong, U.M. Gösele, *Adv. Mater.* **11** (1999) 1409–1425.
- [24] S. Eftychis, J. Kruse, T. Koukoula, Th. Kehagias, Ph. Komninou, A. Adikimenakis, K. Tsagaraki, M. Androulidaki, P. Tzanetakis, E. Iliopoulos, A. Georgakilas, *J. Cryst. Growth* **442** (2016) 8–13.
- [25] S. Fernández-Garrido, J.K. Zettler, L. Geelhaar, O. Brandt, *Nano Lett.* **15** (2015) 1930–1937.
- [26] J.K. Zettler, Ch. Hauswald, P. Corfdir, M. Musolino, L. Geelhaar, H. Riechert, O. Brandt, S. Fernández-Garrido, *Cryst. Growth Des.* **15** (2015) 8.
- [27] A. Fontcuberta i Morral, C. Colombo, G. Abstreiter, *Appl. Phys. Lett.* **92** (2008) 063112.
- [28] T. Aschenbrenner, K. Goepel, C. Kruse, S. Figge, D. Hommel, *Phys. Stat. Sol. (c)* **5** (2008) 1836–1838.
- [29] F. Oehler, A. Cattoni, A. Scaccabarozzi, G. Patriarche, F. Glas, J-C. Harmand, *Nano Lett.* **18** (2018) 701–708.

- [30] A. Concordel, G. Jacopin, B. Gayral, N. Garro, A. Cros, J.-L. Rouviere, B. Daudin, *Appl. Phys. Lett.* **114** (2019) 17210.
- [31] A. Minj, A. Cros, N. Garro, J. Colchero, T. Auzelle, B. Daudin, *Nano Lett.* **15** (2015) 6770–6776.
- [32] J. Zúñiga-Pérez, V. Consonni, L. Lymperakis, X. Kong, A. Trampert, S. Fernández-Garrido, O. Brandt, H. Renevier, S. Keller, K. Hestroffer, M.R. Wagner, J.S. Reparaz, F. Akyol, S. Rajan, S. Rennesson, T. Palacios, G. Feuillet, *Appl. Phys. Rev.* **3** (2016) 041303.
- [33] Y. Morita, K. Miki, H. Tokumoto, *Jpn. J. Appl. Phys.* **30** (1991) 3570–3574.
- [34] J.M.C. Thornton, R.H. Williams, *Semicond. Sci. Technol.* **4** (1989) 847.
- [35] T. Takahagi, I. Nagai, A. Ishitani, H. Kuroda, Y. Nagasawa, *J. Appl. Phys.* **64** (1988) 3516.
- [36] K. Hestroffer, C. Leclere, C. Bougerol, H. Renevier, B. Daudin, *Phys. Rev. B.* **84** (2011) 245302.
- [37] K. Hestroffer, B. Daudin, *Phys. Status Solidi RRL* **7** (2013) 835–839.
- [38] L. Largeau, D.L. Dheeraj, M. Tchernycheva, G.E. Cirlin, J.C. Harmand, *Nanotechnology* **19** (2008) 155704.
- [39] F. Furtmayr, M. Vielemeyer, M. Stutzmann, J. Arbiol, S. Estradé, F. Peirò, J.R. Morante, M. Eickhoff, *J. Appl. Phys.* **104** (2008) 034309.
- [40] F. Furtmayr, M. Vielemeyer, M. Stutzmann, A. Laufer, B.K. Meyer, M. Eickhoff, *J. Appl. Phys.* **104** (2008) 074309.
- [41] H. Sun, X. Li, *Phys. Status Solidi A* **216** (2019) 1800420.
- [42] N. Newman, *J. Cryst. Growth* **178** (1997) 102.
- [43] A.J. Ptak, M.R. Millecchia, T.H. Myers, K.S. Ziemer, C.D. Stinespring, *Appl. Phys. Lett.* **74** (1999) 3836.
- [44] T.H. Myers, M.R. Millecchia, A.J. Ptak, K.S. Ziemer, C.D. Stinespring, *J. Vac. Sci. Technol. B* **17** (1999) 1654.



dr. Marta Sobańska